

FAILURE MODEL OF TEXTURED POLYCRYSTALLINE METALS

Sergiy Kotrechko, Nataliya Stetsenko, and Sergiy Shevchenko

G.V. Kurdyumov Institute for Metal Physics, National Academy of Sciences of Ukraine,
Kyiv, Ukraine
nnst@imp.kiev.ua

Abstract

The effect of crystallographic texture smearing on the anisotropy of the fracture stress of metals was analyzed in this work. It was determined that texture smearing leads to an appreciable decrease in the value of the coefficient of cleavage-stress anisotropy compared to that for metals with very sharp textures. The magnitude of the effect also depends on the prior plastic strain (through its effect on the breadth of texture component) and the level of stress triaxiality.

Keywords: cleavage-stress anisotropy; texture smearing; triaxial stress state

Introduction

The cleavage fracture stress of metal single crystals depends on orientation and may show a marked anisotropy. A corresponding cleavage fracture stress anisotropy in *polycrystalline* metals and alloys may result as well from the development of crystallographic texture during processes such as rolling, drawing, forging, etc. Such an anisotropy can have an important influence on structural integrity. A physics-based model of the anisotropy of the cleavage-stress of polycrystalline metals based on an examination of the elements of cleavage-fracture initiation in polycrystals was developed in [1]. Strictly speaking, this prior analysis is applicable only for very sharp textures that are rarely found in real metals and alloys. Even after very large reductions (~99%), texture smearing exists. In general, the magnitude of smearing (in terms of the texture-component half-width) depends on the value of the imposed plastic strain. Therefore, it is of great practical interest to quantify how such smearing (and, hence, plastic strain) affect the anisotropy of the cleavage-stress.

1. Background

Most types of bulk deformation do not result in the development of a single crystallographic orientation throughout the workpiece, but rather in a range of orientations that characterize its crystallographic texture. The textures that have been most widely investigated are those developed in rolled or rolled-and-recrystallized sheets of materials of cubic crystal symmetry. For example, bcc metals tend to form $\langle 110 \rangle$ -type textures [2]. For *axisymmetric* deformation, such a texture may exhibit a rotational symmetry about the sample axis, i.e., a *fiber* texture [3]. It is usually assumed that the texture of a polycrystalline material rolled to a high reduction will be similar to that developed during rolling to a lower reduction, except that it will be stronger (higher intensity) and sharper (reduced half-width). For example, experimental (111) pole-figure measurements for copper rolled to increasing thickness reductions (35, 58, 82, 90, and 95%) [4] have shown that the texture sharpens with increasing deformation, but the general features remain relatively constant. The same result has been observed for ultra-low carbon steel [5]; increasing the rolling reduction from 70 to 95% increased the maximum intensity of the $\{112\}\langle 110 \rangle$ component markedly.

Textures are usually described by an assembly of discrete orientations or by 2D stereographic projections (pole figures). These are the methods by which texture information is most often obtained and used in practice. For general mathematical analysis as well as for the application of modern orientation image microscopy (OIM), it is often more convenient to represent such

distributions as continuous functions in three-dimensional orientation space, i.e., as orientation distribution functions (ODF) [6], which describe the probability of finding specific texture components as a function of three Euler angles. A general discussion of various forms of ODF has been given in [7]. The sharpness of specific texture components, or conversely the texture smearing, may be quantified by the half-width of Gaussian functions fit to the ODF in 3D Euler space. For example, experimental hot and cold rolling textures of austenitic stainless steel for various reductions (0, 50, 60, 70, and 80%) were presented in [8]. From the data in this paper, it is evident that different processing schedules produce orientations that are distributed in a Gaussian fashion around specific (ideal) texture components in all cases. The half-widths of these distributions decreased to a value of $\sim 8^\circ$ after a rolling reduction of $\sim 80\%$. These and other results based on texture quantification via x-ray diffraction data suggest that texture components are generally Gaussian in shape and exhibit half-widths of the order of 10° or more.

OIM and TEM investigations of the nature of grain-boundary (GB) misorientations provide additional physical insight into the source of texture smearing. In general, a fraction of high-angle GBs exists in polycrystalline metals even after very large deformations. Obviously, the minimum breadth of texture component can not be less than the maximum GB misorientation angle. As has been shown in many investigations, the angle specifying the transition from low-angle to high-angle boundaries is usually between 10 and 15° . For example, it has been found experimentally [9] that the transition from low-angle to high-angle boundaries occurs at $13.6 \pm 0.55^\circ$ in aluminum in the case of symmetric boundaries of rotation around the (112) direction. Thus, it may be concluded that typical textures must have a half-width of at least $10\text{--}15^\circ$ for at least one Euler angle in order for there to be high-angle boundaries within the polycrystalline material. Sharper textures may form only via very special deformation processing schedules or by heat treatments, such as long-time annealing cycles, whose objective is to grow monocrystals.

Evidently, *one of the main reasons* for existence of non-zero minimum value of the breadth of texture component (as well as for existence of grain-boundary (GB) misorientations in highly deformed polycrystal) is deviation of micro-stress state characteristics of separate grains from the corresponding parameters of macro-stress state of polycrystalline aggregate. It is known that at uniaxial tension of polycrystal, its separate grains are under the triaxial stress state, which parameters change stochastically at transition from one grain to another. This gives rise to spread in values of plastic shears in different grains and, hence, to the spread in values of their rotations.

Rolled sheets and plates may show a test-directional dependence of the cleavage-stress; i.e., the fracture stress in tension may be significantly different along the rolling direction compared to its value along the through-thickness direction. For example, experimental data for microalloyed steels [10-12] have shown that the ratio of the fracture stress in rolling direction to that in the through-thickness direction is not large ($\sim 1.2 - 1.3$). On the other hand, theoretical calculations [1] have suggested that this ratio should be ~ 2 . One source of such a difference between theoretical predictions and experimental data may be the fact that texture smearing was not taken into account. Hence, the objective of this paper was to develop a model for quantifying the effect of texture smearing on the anisotropy of the cleavage-stress in metals.

2. Cleavage-stress anisotropy model

The model proposed here is based on the fundamental aspects of cleavage fracture of metals. Specifically, the model postulates that cleavage fracture initiates when the crack nucleus becomes unstable and starts to undergo fast growth. The crack nucleus forms as a result of applied external loading. Its size depends on microstructural features (e.g., ferrite grain size, carbide particle, etc. in steels), that may have a first-order influence on the magnitude of the cleavage-stress.

It is assumed that crack nuclei open on specific crystallographic planes. Thus, the orientation of the critical crack nucleus predetermines the effect of the crystallographic texture on fracture. In other words, the critical stress for the crack nucleus to become unstable depends on the angle between the (crystallographic) crack opening plane and the direction of applied loading. Thus, the smearing and inhomogeneous distribution of crystallographic orientations in real metals may exert an important influence on the anisotropy of the cleavage-stress relations of the model

1. It is assumed that an arbitrarily oriented crack nucleus becomes unstable if:

$$\sigma_1^C \geq f \sigma_C \quad (1)$$

Here, σ_C is the critical (Griffith) stress for the crack nucleus (*oriented normal to the applied stress under uniaxial tension loading*) to become unstable, and f given by the expression [1]:

$$f = \frac{-\beta[1 + L_1\chi] + \sqrt{\beta^2[L_1\chi + 1]^2 - [1 + L_1^2][\beta^2(1 - \chi) - 1]}}{L_{nt}^2(1 + L_1^2)} \quad (2)$$

is a parameter that characterizes the effect of the crack nucleus orientation on the critical tensile stress required for fast crack nucleus growth; $L_1 = l_{s1}/l_{n1}$, l_{n1} and l_{s1} are direction cosines describing the orientation of the applied tensile stress σ_1 relative to crystal coordinate system (\bar{n} is normal to the crack nucleus plane, \bar{s} is normal to the crack frontal line) (Figure illustrating crack nucleation see [1]); $\beta = \bar{\sigma}/\sigma_C$, $\chi = \bar{\tau}/\sigma$ are relative values of the normal and shear dislocation micro-stresses acting on the crack nucleus.

2. The ratio of cleavage-stress values determined in two mutually perpendicular directions was suggested as the coefficient of cleavage-stress anisotropy in [1]. If micro-stress fluctuations are neglected, i.e. *micro- and macroscopic stresses are supposed to be equal*, then, as a first approximation, a coefficient describing the anisotropy of the cleavage-stress can be defined as follows:

$$\gamma_R = \frac{(\sigma_1^C)_I}{(\sigma_1^C)_{II}} \quad (3)$$

in which $(\sigma_1^C)_I$ and $(\sigma_1^C)_{II}$ are the values of the critical microscopic stress for the unstable growth of the crack nucleus in a sample tested in tension along two different directions and assuming a fixed cleavage plane. Combining Equations (1) and (2), the following relation is thus obtained:

$$\gamma_R \approx \frac{f_I}{f_{II}} \quad (4)$$

Equation (4) indicates that the orientation relative to the tension axis of the crystallographic plane on which crack nucleation occurs is the main reason for the anisotropy of the cleavage-stress in textured metals.

3. Relation between the magnitude of texture-component breadth and γ_R for a fiber texture

As was shown in [13], the breadth of the Gaussian fit describing the principal texture components developed during deformation depends on the imposed plastic strain (Fig. 1). In a

prior analysis [1], the effect on γ_R of a sharp axial texture with a [110] fiber axis, such as is developed in drawn wires of cubic metals, was established. In this previous work, the macroscopic stress state was assumed to be uniaxial tension.

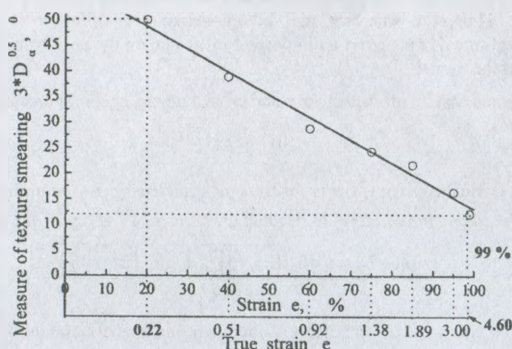


Fig. 1: Breadth of texture component dependence on the plastic strain. D_{α} denotes the variance of the breadth of texture component; $\alpha_{min}^* \approx 12^{\circ}$ is α^* at a plastic strain of ~4.6 (O denote experimental data [13]).

The coefficient of cleavage-stress anisotropy, γ_R , for an axial (fiber) texture can be estimated as the ratio of the critical stress to form the unstable crack nucleus during tension along the [110] fiber-axis direction to the minimum value of this stress which is found for tensile loading along a direction normal to the fiber axis [1]. From Equation (3), γ_R is thus:

$$\gamma_R = \frac{(\sigma_1^C)_{[110]}}{(\sigma_1^C)_{[1\bar{1}2]}} \quad (5)$$

in which $(\sigma_1^C)_{[110]}$ and $(\sigma_1^C)_{[1\bar{1}2]}$ are the values of the critical micro-stress for the formation of the unstable crack nucleus during tension testing of the polycrystalline sample along the [110] and $[1\bar{1}2]$ directions, respectively. The $[1\bar{1}2]$ direction is chosen for the transverse direction because calculations show that among directions lying perpendicular to the [110] fiber axis, $[1\bar{1}2]$ and $[\bar{1}1\bar{2}]$ are those at which the critical stress reaches its minimum value (Fig.2). Neglecting the micro-stress values in the Equation (2) (i.e. if $\beta = 0$ and $\chi = 0$), and supposing the crack nucleus to be susceptible only to normal stresses ($L_1 = 0$ [1]), it is found that $\sigma_{1C}^{[110]} = 4.00 \sigma_C$ and $\sigma_1^{[1\bar{1}2]} = \sigma_1^{[11\bar{2}]} \approx 1.33 \sigma_C$, in which σ_C denotes the value of the critical (Griffith) stress for the initiation of unstable growth of a crack lying in a plane normal to direction of the applied tension stress. Substituting these values into Equation (5), one obtains $\gamma_R \approx 3$. For a cubic material, this is the maximum possible theoretical value of the anisotropy coefficient γ_R for the case when the texture is sharp.

As is well known, cleavage fracture obeys a "weakest-link" principle [14]. In the present case, this means that the crack nucleus will form on a macroscopic (sample) plane most favorably oriented relative to the applied tensile stress and which also contains grains whose

cleavage plane is parallel to this specimen plane. For a material with a fiber texture, the macroscopic plane is thus a function of the maximum fiber component breadth α^* .

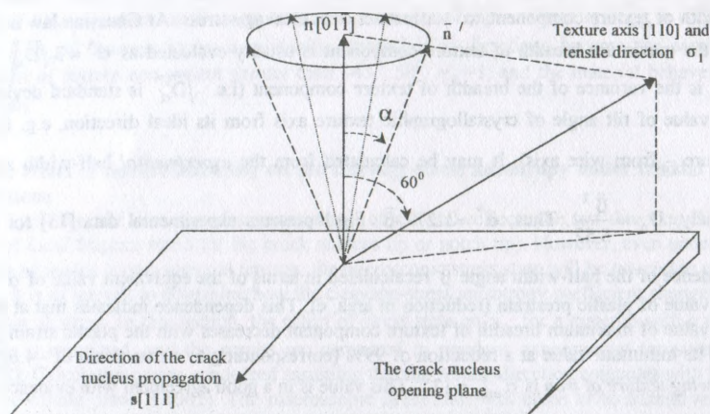


Figure 2: Relation between texture smearing and spread of the orientation of the crack-nucleus opening plane; \bar{s} and \bar{n} denote the direction of crack propagation and the normal to the slip plane.

Inasmuch as each crack nucleus opens on a plane in a given crystallographic family (e.g., $\{01\bar{1}\}$ planes for bcc crystals), which are unambiguously dependent on the texture relative to the imposed loading axis, then texture-component smearing results in a spread of the crack nuclei opening planes (Fig. 2). It means that smearing of texture influences critical cleavage-stress via approaching the crack plane orientation to its most favourable position. This is the physical nature of the texture smearing effect on the value of cleavage-stress anisotropy. The locus of the normals to the crack nucleus plane, \bar{n}' , comprises a cone with a half-angle α around the direction of the fiber \bar{n} $[01\bar{1}]$. Because the critical stress associated with instability of the crack nucleus, σ_1^C , depends on the angle between the normal to the crack-nucleus plane and the tensile axis σ_1 $[110]$, then the value of σ_1^C is different for different positions of the normal, \bar{n}' . As was mentioned above, γ_R is usually estimated by determining only the *minimum* value of σ_1^C in mutually perpendicular directions. For real materials with smeared textures, calculations show that σ_1^C reaches its *minimum* when the scattered normal \bar{n}' , “ideal” (initial) normal \bar{n} $[01\bar{1}]$, and tension axis σ_1 $[110]$ are situated in the *same* plane, thus leading to a minimum angle between \bar{n}' and σ_1 . Therefore, a deviation of the texture axis from the direction $[110]$ by the angle α in the plane $(\bar{n}, \bar{n}', \sigma_1)$ gives rise to a deviation of the normal to the crack plane by the same angle in the same plane, i.e. to an equivalent deviation of the orientation of the crack nucleation plane. Thus, the influence of texture smearing on the value of the coefficient γ_R is due to deviations of the orientations of the crack-nucleation planes. Here, the smearing angles of the normal to the most favourably oriented cracks are equal to the maximum breadth of texture component, α^* , for an axial fiber texture.

Therefore, the effect of texture smearing on γ_R relies on examining the smearing of normals to the crack nucleation planes.

The "weakest-link" principle also implies that *not average but maximum value* of the breadth of texture component, α^* , affects critical cleavage-stress. At Gaussian law of smearing the maximum breadth of texture component is usually evaluated as $\alpha^* \approx 3\sqrt{D_\alpha}$, where D_α is the variance of the breadth of texture component (i.e. $\sqrt{D_\alpha}$ is standard deviation of the value of tilt angle of crystallographic texture axis from its ideal direction, e.g. for axial texture – from wire axis). It may be calculated from the *experimental* half-width angle $\bar{\beta}$, namely, $D_\alpha \approx \frac{\bar{\beta}^2}{5.52}$. Thus, $\alpha^* \approx 1.277 \cdot \bar{\beta}$. Fig.1 presents experimental data [13] for the de-

pendence of the half-width angle $\bar{\beta}$ recalculated in terms of the equivalent value of α^* (e) on the value of plastic prestrain (reduction in area, e). This dependence indicates that at drawing the value of maximum breadth of texture component decreases with the plastic strain growth, and its minimum value at a reduction of 99% (corresponding to a true strain of -4.6) for the *drawing texture of iron* is $\alpha_{\min}^* \approx 12^\circ$. This value is in a good agreement with evidence in [9].

Computer calculations were performed to determine γ_R from Equation (5) for different breadths of texture component. The results, shown in Fig. 3, demonstrate that the effect of plastic strain on the breadth of texture component produces a decrease in γ_R of at least one-third relative to the value of γ_R for a sharp texture (i.e., $3 \rightarrow 2$). However, the existence of a minimum value of maximum breadth of texture component α_{\min}^* ($\approx 12^\circ$) enables the determination of the maximum contribution of crystallographic texture to the value of γ_R . The calculations (Fig. 3) reveal that this amounts to a factor of ~ 2 for the drawing textures under consideration; i.e., γ_R varies from 2 to 1 as the breadth of texture component increases.

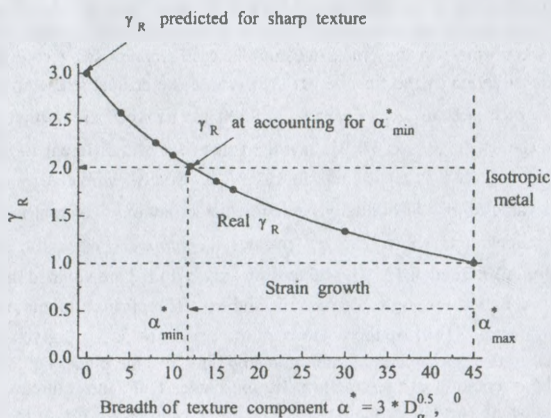


Fig. 3: Effect of texture smearing on the value of γ_R . γ_R predicted for sharp texture is the maximum contribution of crystallographic texture to the value of γ_R .

In practice, the value of $\gamma_R \sim 2$ represents an *upper bound*. The actual value will be less than 2 because of the breadth of texture component dependence on strain level (Fig. 1). The breadth of texture component grows with decreasing in the value of wire upset, so the coefficient of cleavage-stress anisotropy decreases. Estimations indicate that at $\alpha_{\min}^* \approx 45^\circ \dots 50^\circ$ the values of cleavage-stress in mutually perpendicular directions become the same. For breadths of texture component greater than $\sim 45 \dots 50^\circ$, $\gamma_R = 1$, and the material behaves isotropically.

4. The effect of texture smearing on the cleavage-stress anisotropy under triaxial stress conditions

Typically, the cleavage-stress anisotropy of a metal reflects the test-direction dependence of *local* fracture stress (at the crack nucleus tip or notch tip). However, even under conditions of *macro*-scopic uniaxial tension, the *microscopic* stress state will be *triaxial* in nature. Thus, it is of interest to determine how the cleavage-stress anisotropy coefficient changes with the state of stress. In this section, the effect of stress state on γ_R for a material with a rolling texture is examined, and the results are compared to previous experimental measurements [10-12]. Calculations were conducted assuming that the rolling direction coincides with [110], and the rolling plane is (001). The macroscopic stress state was taken to be triaxial tension. Let us estimate the effect of triaxiality taking as an example rolling plate with Charpy notch. There are two limit cases, namely, when maximum tensile stress at the notch tip, σ_1 , coincides with through-thickness direction (the first case), and when this stress is oriented transversely to rolling direction (the second case).

As a first example, calculations were conducted for the case of a sharp texture ($\alpha = 0$) and different values of the stress ratio $\eta_{21} = \sigma_2/\sigma_1$ for a given value of $\eta_{31} = \sigma_3/\sigma_1 \approx 0.41$ (Fig.4). The results in Fig.4 show that γ_R decreases as η_{21} increases. In particular, for $\eta_{21} \approx 0.7 - 0.8$, $\eta_{31} \approx 0.41$, or stress-state parameters that typify the loading conditions ahead of the notch in Charpy tests [11], the magnitude of γ_R was predicted to lie between approximately 1.06 and 1.12. These values are similar to those found experimentally. Certain exceeding of experimental evidence over the calculation results may, possibly, be due to micro-stress effect (at evaluations parameters β and χ in (2) were neglected). The decrease in the magnitude of γ_R may be explained using Equation (5) and explicit expressions for $(\sigma_i^C)_{[110]}$ and $(\sigma_i^C)_{[112]}$ for the case of triaxial tension. Substituting these expressions into Equation (5), the following is obtained:

$$\gamma_R = \frac{(l_{n2}/l_{n1})^2 + \eta_{21}(l_{n3}/l_{n1})^2 + \eta_{31}}{1 + \eta_{21}(l_{n2}/l_{n1})^2 + \eta_{31}(l_{n3}/l_{n1})^2} \quad (6)$$

For a fixed value of η_{31} (it should be kept in mind that in mechanics η_{21} is *generally accepted to be greater or equal than* η_{31}), the dependence of γ_R on the parameter η_{21} is of the following form, therefore:

$$\gamma_R(\eta_{21}) = \frac{a\eta_{21} + b}{c\eta_{21} + d}, \quad (7)$$

where

$$a = (l_{n3}/l_{n1})^2, \quad b = (l_{n2}/l_{n1})^2 + \eta_{31}, \quad c = (l_{n2}/l_{n1})^2, \quad d = 1 + \eta_{31}(l_{n3}/l_{n1})^2 \quad (8)$$

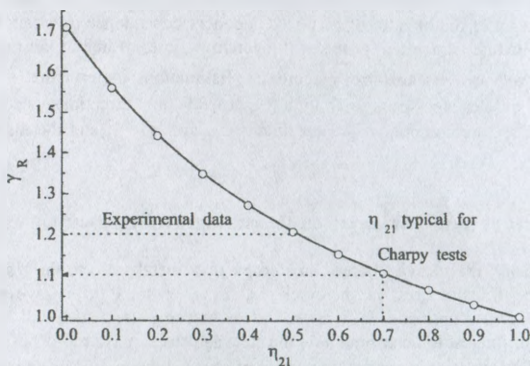


Fig. 4. Dependence of the cleavage-stress anisotropy coefficient, γ_R , on the parameters of multiaxial stress state $\eta_{21} = \sigma_2/\sigma_1$, $\eta_{31} = \sigma_3/\sigma_1$ for the case of a sharp rolling texture, ($\eta_{31} = 0.41$).

Expressions similar to Equations (6) and (7) may also be derived for the case, in which η_{21} is constant. In addition, a relatively simple analysis based on Equation (6) shows that γ_R decreases monotonically with increases in the (independent-variable) stress ratio in both cases. The maximum value of γ_R equals approximately 2 at $\eta_{31} = \eta_{21} = 0$ (for rolling texture) and has a minimum value of exactly unity for $\eta_{31} = \eta_{21} = 1$, i.e., for $\sigma_1 = \sigma_2 = \sigma_3$ (this is lower bound because accounting of the micro-stress effect increases γ_R). The latter is evident because at the *uniform* triaxial tension ($\sigma_1 = \sigma_2 = \sigma_3$) stress field is symmetric. It means that at an arbitrary crack nucleus orientation, which is specified by crystallographic texture parameters, the magnitude of normal stresses, acting on the crack nucleus, is the same.

It should also be noted that dependences identical to those for $\eta_{31} = 0.41$ are obtained for any value η_{31} in the range $0 \leq \eta_{31} \leq 1$. The only difference is that the specific curve relating γ_R and η_{21} is situated higher (for $\eta_{31} \leq 0.41$) or lower (for $\eta_{31} \geq 0.41$) than that given in Fig. 4.

Above results are obtained for perfectly sharp texture. It is of practical interest to predict how the texture smearing influences dependence of anisotropy coefficient on the triaxial stress state parameters. Fig. 5 summarizes calculations for the cleavage-stress anisotropy γ_R for cases involving both texture smearing (four values of α_{\min}^* are considered) and a triaxial stress state. To simplify calculations, direction [110] was supposed to spread axisymmetrically relatively to its location in sharp texture. The dependence of γ_R on η_{21} for $\alpha \neq 0$ is similar to that for a sharp texture ($\alpha = 0$) shown in Fig. 4. As $\eta_{21} \rightarrow 1$, the difference between the magnitude of γ_R for a sharp texture and textures with various breadths of texture component decreases; i.e., the effect of texture smearing on the cleavage-stress anisotropy decreases. At $\alpha_{\min}^* \approx 45^\circ$, the effect of cleavage-stress anisotropy practically vanishes just as in the case of uniaxial tension (Fig. 3). In fact, under conditions of 'balanced' biaxial or triaxial loading, γ_R is not sensitive to the degree of texture perfection.

This conclusion is of great importance for prediction of structural integrity because experimental finding of the coefficient of cleavage-stress anisotropy using σ_F at the notch tip essentially decreases γ_R . From a practical standpoint, the results in Fig. 5 also suggest that the maximum level of cleavage-stress anisotropy be obtained for conditions characterized by stress states closest to uniaxial tension, i.e. for determination of maximum γ_R values, specimens, where such stress state of metal is realized, should be applied.

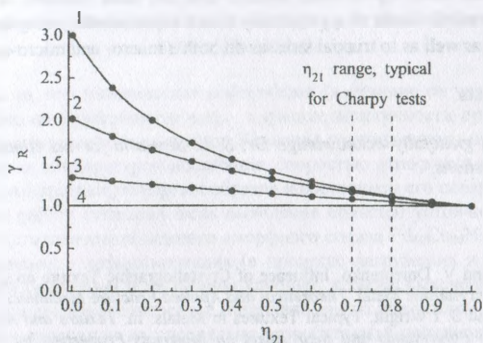


Fig. 5. Simultaneous influence of the breadth of texture component, α^* , and the multiaxial stress state parameters, $\eta_{21} = \sigma_2/\sigma_1$, $\eta_{31} = \sigma_3/\sigma_1$, on the cleavage-stress anisotropy coefficient γ_R

($\eta_{31} = 0.41$): 1 – sharp texture; 2 - $\alpha^* = 12^\circ$; 3 - $\alpha^* = 30^\circ$; 4 - $\alpha^* = 45^\circ$

5. Conclusions

A theoretical investigation of the effect of texture smearing on the anisotropy of the cleavage-stress of metals was conducted. The following conclusions are drawn from this work:

1. Non-uniform distribution of orientations of crystallographic planes where the crack nucleus open is the main reason for cleavage-stress anisotropy of textured polycrystals. Texture smearing gives rise to decrease in the value of coefficient of cleavage-stress anisotropy. For $\alpha_{\text{min}}^* \sim 12^\circ$, the cleavage-stress anisotropy coefficient γ_R under uniaxial tension loading is decreased by a factor of one-third relative to that for a perfectly-sharp texture.
2. The magnitude of the coefficient of cleavage-stress anisotropy depends on the maximum value of the breadth of texture component α^* ($\alpha^* = 3\sqrt{D_\alpha}$, where D_α is the variance of breadths of texture component).
3. The breadth of texture component, α^* , typically found in drawn metals (axial or drawing texture) decreases to its minimum value of approximately $\alpha_{\text{min}}^* \sim 10-15^\circ$ (this is the lower bound of α^*), as the imposed deformation is increased from 0.2 to 4.6. Here, exceeding of cleavage-stress measured along the wire axis may be twofold relatively to those measured in transverse direction due to crystallographic texture. At $\alpha^* \approx 45^\circ$ effect of cleavage-stress anisotropy vanishes.
4. A triaxial stress state also significantly decreases the value of the coefficient of cleavage-

stress anisotropy γ_R in comparison to its value under conditions of uniaxial tension. This is due to the growth of stress field symmetry. The effect of texture smearing on γ_R decreases to zero as the stress state approaches a state consisting of balanced biaxial stress or purely hydrostatic stress. At the uniform triaxial tension ($\sigma_1 = \sigma_2 = \sigma_3$) the coefficient of cleavage-stress anisotropy owing to crystallographic texture $\gamma_R \rightarrow 1$. By virtue of above mentioned, the level of cleavage-stress anisotropy determined by the data on local cleavage-stress at the notch tip is much smaller than the same obtained at uniaxial tension. Therefore, the small values of γ_R typically found experimentally may be attributed to texture smearing as well as to triaxial stresses on both a macro- and micro-scale.

Acknowledgements

The authors gratefully acknowledge Dr. S. L. Semiatin for his stimulating discussions and helpful suggestions.

References

1. S. Kotrechko and V. Dniprenko, Influence of Crystallographic Texture on Cleavage Stress Anisotropy of Polycrystalline Metal. *Theoretical and Applied Fracture Mechanics*. 2003, in press
2. A. D. Rollet and S. I Wright, Typical Textures in Metals. In: *Texture and Anisotropy: Preferred Orientations in Polycrystals and their Effect on Materials Properties*, by U. F. Kocks, C. N. Tomé, H. R. Wenk. Cambridge University Press, 2000.
3. H.-J. Bunge, *Texture Analysis in Material Science – Mathematical Methods*. London: Butterworth, 1982.
4. C. T. Necker, Recrystallization Texture in Cold Rolled Copper. Ph.D. Thesis (Philadelphia Pa. Drexel University), 1997.
5. K. Verbeken, L. Kestens, J. J. Jonas, Microtextural Study of Orientation Change During Nucleation and Growth in a Cold Rolled ULC Steel. *Scripta Mater*. Vol 48, pp 1457-1462, 2003.
6. F. Bitter, *Introduction to Ferromagnetism*. New York: McGraw-Hill, 1937.
7. H. Schaeben, Parameterization and Probability Distributions of Orientations. *Texture Microstruct*. Vol. 13, pp. 51-54, 1990.
8. D. Raabe, Texture and Microstructure Evolution During Cold Rolling of a Strip Cast and of a Hot Rolled Austenitic Stainless Steels. *Acta Mater*. Vol 45, No. 3, pp.1137-1151, 1997.
9. M. Winning, G. Gottstein, L.S. Shvindlerman. On the mechanisms of grain boundary migration. *Acta Materialia*, Vol. 50, pp. 353-364, 2002.
10. B. Dogan and J. D. Boyd, Through-Thickness Fracture of a Ti-V-N Plate Steel. *Metallurgical Transactions A*. Vol. 21A, pp.1177-1191, 1990
11. G. Baldi and G. Buzzichelli, Critical Stress for Delamination Fracture in HSLA Steels, *Metal Science*. Vol. 12, No. 10, pp. 459-472, 1978.
12. J. Sun, J. D. Boyd, Effect of Thermomechanical Processing on Anisotropy of Cleavage Fracture Stress in Microalloyed Linepipe Steels. *International Journal of Pressure Vessels and Piping*. Vol. 77, pp. 369-377, 2000.
13. Yu. Ya. Meshkov T. N. Serditova. Fracture of Deformed Steel, Naukova Dumka, Kiev, 1989 (in Russian).
14. W.A. Weibull. Statistic Theory of Strength of Materials. *Proc.Roy. Swed. Inst Eng. Res.*, 151, 5-12 (1939).